Autophagy in the Aging and Experimental Ocular Hypertensive Mouse Model

April Nettesheim, Angela Dixon, Myoung Sup Shim, Aislyn Coyne, Molly Walsh, and Paloma B. Liton

Department of Ophthalmology, Duke University, Durham, North Carolina, United States

Correspondence: Paloma B. Liton, Duke Eye Center, Duke University, AERI Building, Office 4004, Box 3802, 2351 Erwin Road, Durham, NC 27713, USA;
paloma.liton@duke.edu.

AN and AD contributed equally to the work presented here and should therefore be regarded as equivalent authors.

Received: January 24, 2020
Accepted: July 15, 2020
Published: August 14, 2020

Citation: Nettesheim A, Dixon A, Shim MS, Coyne A, Walsh M, Liton PB. Autophagy in the aging and experimental ocular hypertensive mouse model. *Invest Ophthalmol Vis Sci.* 2020;61(10):31.
https://doi.org/10.1167/iovs.61.10.31

Purpose. To investigate autophagy in the outflow pathway and ganglion cell layer in the aging and ocular hypertensive mouse.

Methods. Both 4-month-old and 18-month-old C57BL/6J and GFP-LC3 mice were subjected to unilateral injection of hypertonic saline into a limbal vein, causing sclerosis of the outflow pathway and subsequent elevation of intraocular pressure (IOP). IOP was measured on a weekly basis using a rebound tonometer. Protein expression levels of LC3B, Lamp1, and p62 were evaluated by western blot and/or immunofluorescence. Retinal ganglion cell (RGC) count was performed in whole retinal flat mounts using an anti-Brn3a antibody. Optic nerves were fixed with 4% paraformaldehyde and resin-embedded for axon counts and electron microscopy.

Results. In contrast to 18-month-old mice, which developed sustained elevated IOP with a single injection, 4-month-old mice were refractory to high elevations of IOP. Interestingly, both the percentage of animals that developed elevated IOP and the mean ΔIOP were significantly higher in the transgenic mice compared to C57BL/6J. Immunofluorescence and western blot analysis showed dysregulated autophagy in the iridocorneal and retina tissues from 18-month-old mice compared to 4-month-old ones. Moreover, the LC3-II/LC3-I ratio correlated with IOP. As expected, injected hypertensive eyes displayed axonal degeneration and RGC death. RGC and axon loss were significantly exacerbated with aging, especially when combined with GFP-LC3 expression. Autophagic structures were observed in the degenerating axons.

Conclusions. Our results indicate dysregulation of autophagy in the trabecular meshwork and retinal tissues with aging and suggest that such dysregulation of autophagy contributes to neurodegeneration in glaucoma.

Keywords: functional MRI, phoria adaptation, reliability, intraclass correlation coefficient, oculomotor vermis

Aging and ocular hypertension are believed to be the two major risk factors associated with the development and progression of primary open-angle glaucoma, a progressive optic neuropathy and second leading cause of permanent blindness worldwide.[1,2] Yet, the mechanisms by which these two factors predispose the disease are far from being understood.

Aging is a complex phenomenon characterized by the continuous accumulation of deleterious changes. These changes result in the gradual decline in both cellular and physiological functions, as well as a diminished capacity to respond to stress, thus increasing the likelihood of degenerative diseases.[3] One of the cellular stress response mechanisms affected by aging is autophagy. Autophagy is the process by which aged or damaged cellular constituents, including organelles, are degraded through the lysosomal compartment. Although autophagy activity is essential to maintaining cell homeostasis, evidence has shown that it is itself affected by aging.[4] Alterations in autophagy with aging have been associated with the onset or progression of age-related diseases,[5–7] including ocular hypertension and glaucoma.[8–14]

Data from our laboratory have demonstrated the dysregulation of autophagy in trabecular meshwork (TM) cells—one of the cell types involved in the regulation of ocular pressure—isolated from glaucoma cadaver eyes,[15] as well as in TM primary cultures subjected to an experimental in vitro model of aging.[16,17] Pulliero et al.[18] evaluated autophagy markers in TM tissue dissected from human cadaver eyes from young and old subjects and found an age-dependent increase in the levels of autophagy markers, which correlated with oxidative DNA damage. Also, treatment with the autophagy inducer rapamycin showed a protective effect against oxidative insult in TM cells.[19] Activation of autophagy has been also reported in retinal ganglion cells (RGCs) in response to injury or in acute and chronic experimental models of elevated intraocular pressure (IOP) in mice, rats, and rhesus monkeys.[20–24] In addition, our group has recently characterized the contribution of autophagy to ocular hypertension and neurodegenera-

tion in the DBA/2J spontaneous glaucoma mouse model.[25] However, no studies so far have evaluated the effect of aging on autophagy activity in the ocular tissues relevant to glaucoma in mice.

In this work, we have compared autophagy in the iridocorneal angle region, RGC bodies, and optic nerve (ON) axons from 4-month-old and 18-month-old normotensive and ocular hypertensive mice. Our results indicate dysregulated autophagy in the TM and RGCs with aging and with experimental ocular hypertension.

Methods

Animal Husbandry, Genotyping, and Tissue Collection

Transgenic green fluorescent protein (GFP)-LC3 mice were obtained and genotyped, as previously described.[25] GFP-LC3 mice were maintained and bred as heterozygous and aged in situ. Homozygous and littermate wild-types (males and females, 4 months old and 18 months old) were used for experimental purposes. Animals were maintained under a 12-hour light/dark cycle, fed a standard mouse diet, and provided with water ad libitum. Animal euthanasia was performed via CO_2 asphyxiation, followed by bilateral thoracotomy, prior to immediate enucleation. Enucleated eyes destined for immunofluorescence (IF) were fixed with 4% paraformaldehyde (PFA). Tissues destined for western blot (WB) analysis were immediately dissected and flash frozen on dry ice. Optic nerves were fixed in 4% PFA/1% glutaraldehyde/0.12-M phosphate buffer and processed for plastic sections and electron microscopy, as described below. All procedures were reviewed and approved by the Institutional Animal Care and Use Committee of Duke University and were performed in accordance with the ARVO Statement for the Use of Animals in Ophthalmic and Vision Research and the National Institutes of Health Guide for the Care and Use of Laboratory Animals.

Chronic Ocular Hypertensive Model

Chronic elevation of IOP was established via a modified version of Morrison's model adapted to mice.[26–28] The model consists of injecting hypertonic saline into a limbal vein, causing sclerosis of aqueous outflow channels and a subsequent elevation of IOP. For this, a modified plastic occlusion ring was placed around the equator of the eye, and a pulled glass micropipette was carefully inserted into an episcleral vein near the cornea of anesthetized mice (ketamine, 100 mg/kg; xylazine, 5–10 mg/kg). Immediately after cannulation, a volume of 0.05 cc of sterile 1.3-M saline was injected into the limbal venous system. Unilateral injections were performed. The contralateral non-injected eye was used as control. Up to three injections 2 weeks apart were conducted as required to elevate IOP. IOP was measured postoperatively on a weekly basis as described below. Animals were euthanized and tissue was collected 6 weeks after initial IOP elevation.

IOP Measurements

Diurnal IOP measurements were taken between 10 AM and 12 PM in anesthetized animals (ketamine, 100 mg/kg; xylazine, 5–10 mg/kg) using a TonoLab rebound tonometer (Colonial Medical Supply, Franconia, NH, USA), as previously described.[25] IOP was measured on a monthly basis for aging studies and on a weekly basis postoperatively in the ocular hypertensive mice. Six measurements, taken within 5 minutes after anesthesia, were collected per eye. These values were averaged to produce a single IOP value per eye for each measurement session. While the mice were anesthetized, their body temperature was maintained at 38°C to 40°C by using Deltaphase isothermal pads (Braintree Scientific, Inc., Braintree, MA, USA). Integral IOP (cumulative pressure received by each mouse for the entire duration of the experiment) was calculated using the area under the curve (AUC) tool of Prism 5 software (GraphPad, San Diego, CA, USA), and expressed as mm Hg-days. The integral IOP difference (ΔIntegral IOP = Integral $IOP_{injected}$ − Integral $IOP_{uninjected}$) was used as a measure of IOP exposure in the injected compared to the uninjected eye for each animal.

Protein Whole-Tissue Lysates and Western Blot

Protein whole-tissue lysates were prepared as previously described.[25] Briefly, the dissected tissue was homogenized by manual grinding in cold radioimmunoprecipitation assay (RIPA) buffer containing protease inhibitor cocktails (Thermo Fisher Scientific, Waltham, MA, USA) and molecular grinding resin (G-Biosciences, St. Louis, MO, USA). Lysates were subjected to three freeze/thaw cycles and clarified by centrifugation at 12,000*g* for 30 minutes at 4°C. Protein concentration was determined using the Micro BCA Protein Assay Kit (Thermo Fisher Scientific). Protein lysates (5 µg) were separated in 15% polyacrylamide SDS-PAGE gels and transferred to polyvinylidene fluoride membranes (Bio-Rad Laboratories, Hercules, CA, USA). Membranes were blocked with 5% non-fat dry milk in 0.1% Tween-20/Tris-buffered saline (TBS) and incubated overnight with anti-LC3 antibody (NB100-2331; Novus Biologicals, Littleton, CO, USA) or anti β-Actin (sc-69879; Santa Cruz Biotechnology, Santa Cruz, CA, USA). The bands were detected by incubation with a secondary antibody conjugated to a horseradish peroxidase and chemiluminescence substrate (ECL Western Blotting Detection Reagents, GE Healthcare, Chicago, IL, USA; Pierce ECL 2, Thermo Fisher Scientific). Blots were scanned and analyzed by densitometry using Image J (National Institutes of Health, Bethesda, MD). Relative quantification of LC3 protein levels was calculated using β-actin as the loading control.

Immunofluorescence on Frozen Sections

Tissue samples were fixed in 4% PFA, cryopreserved, and sectioned as previously described.[25] For immunolabeling, sections were permeabilized with 0.5% Triton-X/PBS for 10 minutes at room temperature and incubated in 2% BSA/5% normal goat serum/0.1% Triton-X/PBS for 30 minutes at room temperature to block non-specific sites. Samples were then incubated overnight at 4°C with primary antibodies diluted in a blocking solution of anti-LC3 (PM036; MBL International, Woburn, MA, USA), anti-p62 (P0067; Sigma-Aldrich, St. Louis, MO, USA), and anti-LAMP1 (ab24170; Abcam, Cambridge, UK). After a series of washes with 1× PBS, samples were incubated for 1 hour at room temperature in Alexa Fluor 568 Goat anti-Rabbit antibody (Thermo Fisher Scientific) diluted 1:1000 in serum-free blocking solution. Nuclei were counterstained with DAPI (1:1000 in PBS). Images were collected using a Nikon

TE2000 confocal microscope with a 60× objective (Nikon Corporation, Tokyo, Japan). All tissues were immunostained at the same time, and images were captured the same day under the same laser settings to avoid interexperimental variability. Anterior segment sections were graded in a masked fashion by three independent observers, and mean scoring values of IF staining in the TM/SC region were calculated. Standardized relative quantification of immunofluorescence staining in the RGC layer was calculated using Image J as described in Hirt et al.[25]

Whole Retinal Flat Mounts and RGC Count

Quantification of peripheral RGC density was performed in whole flat-mount retinas. For this, retinal tissues from eyes fixed in 4% PFA were dissected and flat-mounted. Tissues were then washed three times for 10 minutes in 0.5% Triton-X/1× PBS at room temperature and permeabilized overnight in 2% Triton-X/1× PBS at 4°C with agitation. Retinas were subsequently incubated for 3 days at 4°C with anti-Brn3a antibody (1:750 in 2% Triton-X/2% normal donkey serum/1× PBS; Santa Cruz Biotechnology). After a series of washes in permeabilization buffer, retinas were incubated at room temperature for 4 hours with Alexa Fluor 568 Donkey anti-Goat antibody (1:500 in permeabilization buffer; Thermo Fisher Scientific) and counterstained in 4′,6-diamidino-2-phenylindole (DAPI, 1:1000 in 0.5% Triton-X/1× PBS) for 30 minutes at room temperature. Samples were then washed in 0.5% Triton-X/1× PBS, mounted in Fluoromount G aqueous mounting media (Electron Microscopy Sciences, Hatfield, PA, USA) and coverslipped. Retinal flat mounts were imaged using an Nikon TE2000 confocal microscope with a 40× objective and the EZ-C1.3.10 software. A series of four images were taken at equidistant points along the peripheral circumference of the retina. Brn3a-positive cells were quantified and averaged using a custom semi-automatic application developed for MATLAB (MathWorks, Natick, MA, USA) which identified RGCs based on color, shape, and size.

Optic Nerve Axon Count

Optic nerves were dissected from underneath the brain, fixed overnight in 4% PFA/1% glutaraldehyde in 0.12-M phosphate buffer, and subsequently embedded in the Embed-812 resin mixture (Electron Microscopy Science). ONs were sectioned approximately 3 to 5 mm distal of the optic nerve head at a thickness of 300 nm on a Leica EM UC6 ultramicrotome (Leica Camera, Wetzlar, Germany) using a diamond knife (Histo Diamond Knife, 45°, 4.0-mm; Diatome US, Hatfield, PA, USA). Cross-sections were stained with 1% Toluidine Blue, 1% sodium borate aqueous solution and coverslipped. Axon counts were obtained using the Zeiss AxioVision imaging system. Image analysis consisted of RGB thresholding, followed by size and form factor exclusions. Approximately 40% of the total cross-sectional area for each ON was counted; results were extrapolated to the entire nerve for each mouse.

Electron Microscopy

Optic nerves were dissected and processed as described above. Ultrathin cross-sections were cut at 65 nm-thick using a Leica EM CU7 ultramicrotome and contrast stained with 2% uranyl acetate/4% lead citrate solution. Nerve images were obtained using a JEM-1400 transmission electron microscope (JEOL) equipped with an ORIUS 1000 charge-coupled device (CCD) camera (Gatan, Inc., Pleasanton, CA, USA).

Statistical Analysis

All statistical analyses were performed using GraphPad Prism software. Data are presented as mean values ± SD using the Tukey post hoc test. Statistical significance was calculated using paired Student's *t*-test for two-group comparison, or 2-way ANOVA with Bonferroni post hoc test for multiple groups. $P < 0.05$ was considered statistically significant.

Results

Effect of Aging and GFP-LC3 Transgene Expression in IOP Elevation

We first evaluated the effect of aging and/or GFP-LC3 transgene expression on IOP in normotensive mice. For this, we conducted IOP measurements on a monthly basis in C57BL/6J and transgenic GFP-LC3 mice, which ubiquitously express the autophagosome marker LC3 fused to GFP. As seen in Figure 1A, a progressive increase in mean IOP with aging was observed in both C57BL/6J (r = 74,79%, $P < 0.0001$) and GFP-LC3 (r = 71.81%, $P < 0.001$) mice. No difference in IOP was observed in GFP-LC3 compared to age-matched C57BL/6J control mice, thus confirming our previous data indicating no significant effect of GFP-LC3 transgene on outflow pathway tissue function.[25]

Next, we examined the effect of aging and/or GFP-LC3 transgene expression in experimental chronic ocular hypertensive mice. To generate these, we injected hypertonic saline into a limbal vein of 4-month-old and 18-month-old C57BL/6J and GFP-LC3 mice, as detailed in Methods. This procedure causes sclerosis of aqueous outflow channels and a subsequent elevation of IOP. The ΔIntegral IOP was calculated as a measure of the differential cumulative pressure received for each eye during the 6-week period. A summary of the injections and ΔIntegral IOPs are included in the Table and represented in Figures 1B and 1C. As seen, the majority of the mice within the 4-month-old group did not develop high IOP, defined as ΔIntegral IOP > 50 mm Hg-days even after three rounds of injections. Interestingly, both the percentage of animals developing elevated IOP (41% vs. 27%) and the mean ΔIntegral IOP (73.12 ± 253 vs. −15.92 ± 135.4 mm Hg-days; $P = 0.005$, *t*-test) were slightly higher in the transgenic mice compared to C57BL/6J controls. In contrast to the animals in the 4-month-old group, a single injection was sufficient to induce sustained high elevation in IOP in the majority of the 18-month-old mice (89% and 94% in C57BL/6J and GFP-LC3, respectively). A statistical significance in ΔIntegral IOP was found with aging ($P < 0.0001$, 2-way ANOVA), but not with genotype. Post hoc tests revealed significant higher pairwise ΔIntegral IOP in 18-old-month mice compared to the respective 4-month-old mice ($\Delta IOP_{18mo\text{-}C57BL/6J}$: 292.6 ± 311.3 mm Hg-days vs. $\Delta IOP_{4mo\text{-}C57BL/6J}$: −15.92 ± 135.4 mm Hg-days; $\Delta IOP_{18mo\text{-}GFP\text{-}LC3}$: 309.1± 279.6 mm Hg-days vs. $\Delta IOP_{4mo\text{-}GFP\text{-}LC3}$: 73.12 ± 253.5 mm Hg-days; $P < 0.05$; n sizes are indicated in the Table). Although the percentage of GFP-LC3 mice developing severe levels of ΔIntegral IOP (defined as >200 mm Hg-days) was significantly larger than that of C57BL/6J (65% vs. 44%), we did not observe a

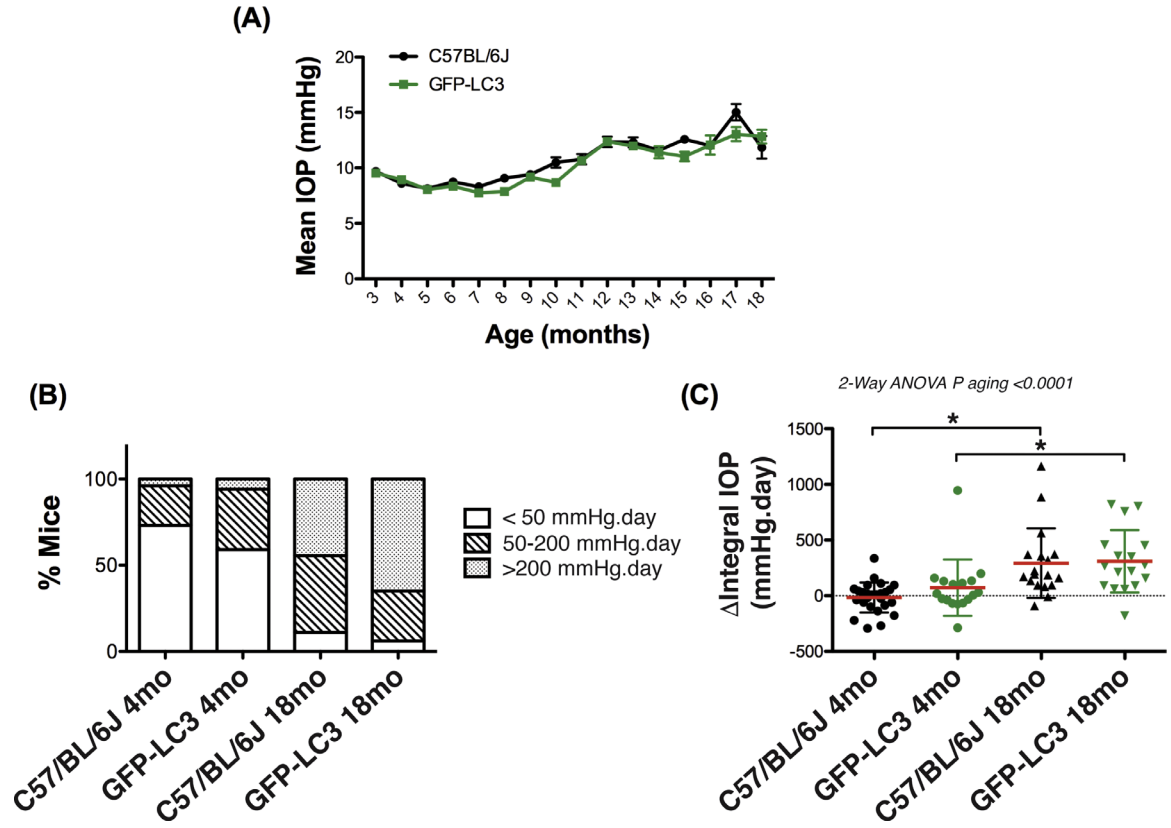

Figure 1. Effect of age and GFP-LC3 transgene on IOP. (**A**) Mean IOP (mm Hg) over time in C57BL/6J and GFP-LC3 mice. (**B**) Percentage of injected mice developing low (<50 mm Hg-days), mild (5–200 mm Hg-days), and severe (>200 mm Hg-days) ΔIntegral IOP. (C) ΔIntegral IOP with aging and GFP-LC3. $^{*}P < 0.05$, 2-way ANOVA with Bonferroni post hoc test ($n_{4moC57BL/6J} = 26$, $n_{18moC57BL/6J} = 17$, $n_{4moGFP\text{-}LC3} = 18$, $n_{18moGFP\text{-}LC3} = 17$).

Table. Summary of Injections and IOP in Ocular Hypertensive Experimental Mice

			Percentage of Mice			
Mice	***n***	**No. of Injections**	**ΔIntegral IOP ≤ 50 mm Hg-days**	**ΔIntegral IOP = 50–200 mm Hg-days**	**ΔIntegral IOP > 200 mm Hg-days**	**ΔIntegral IOP Mean ± SD (mm Hg-days)**
4 months old						
C57BL/6J	26	3	73%	23%	4%	–15.92 ± 135.4
GFP-LC3	17	3	59%	35%	6%	73.12 ± 253.5
18 months old						
C57BL/6J	18	1	11%	45%	44%	292.6 ± 311.3
GFP-LC3	17	1	6%	29%	65%	309.1 ± 279.6

significant difference in the ΔIntegral IOP associated with the transgene expression. Together our results suggest a predisposition to sclerotic lesion or loss in regenerative potential in the aging mice in response to the saline injection.

Autophagy in the Iridocorneal Region of Aging Mice

A decline in autophagy with aging has been reported in other tissues.[4] Our laboratory has also reported dysregulated autophagy in cultured porcine TM cells under chronic oxidative stress,[16,17] as well as in primary cultures of human TM cells isolated from glaucomatous eyes.[15] Autophagy in the aging TM has just been investigated in one study in humans,[18] but never in mice, to the best of our knowledge. To investigate autophagy in the outflow pathway tissue of aging mice, we monitored by WB analysis the levels of the autophagosome marker LC3-II in protein lysates from dissected iridocorneal region of 4-month-old and 18-month-old C57BL6/J mice. Note that for aging studies uninjected eyes were used. As seen in Figure 2A, two bands with molecular weights corresponding to LC3-I (~16 kDa) and LC3-II (~14 kDa) were observed in the iridocorneal region from 18-month-old mice. Two additional bands were recognized by the LC3 antibody in the protein lysates from

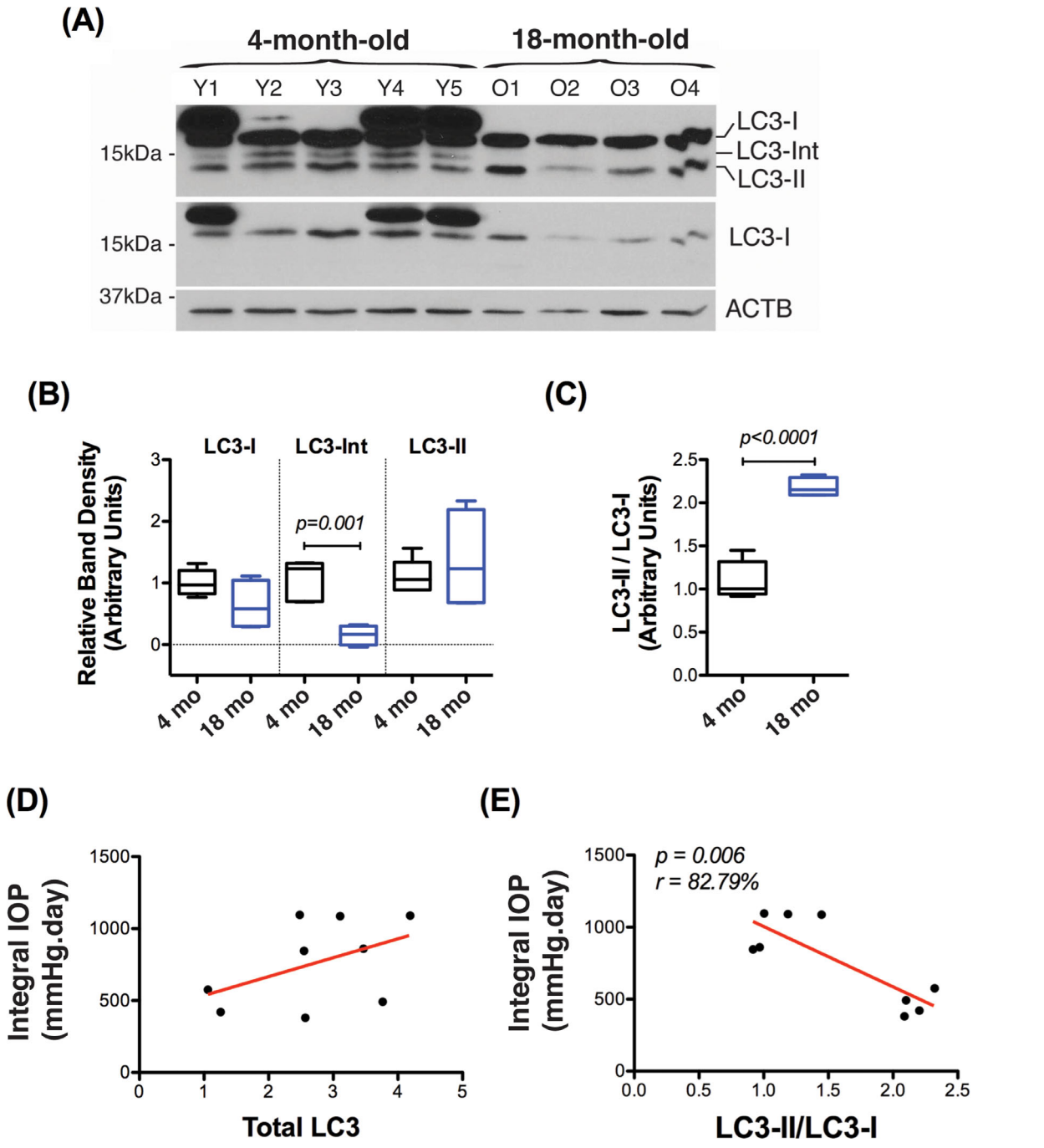

Figure 2. Quantification of the autophagy marker LC3 in the dissected iridocorneal angle region from 4-month-old and 18-month-old C57BL/6J mice. (**A**) Protein expression levels of LC3 in whole-tissue lysates (5 µg) of dissected iridocorneal region from 4-month-old (n = 5) and 18-month-old (n = 4) C57BL/6J mice, analyzed by WB. (**B**) Normalized relative protein levels of LC3-I, LC3-Int, and LC3-II and (**C**) the LC3-II/LC3-I ratios were calculated from the densitometric analysis of the bands. β-Actin was used as a loading control. Data are the means ± SD; t-test. (**D**, **E**) Linear correlation analysis between total LC3 and LC3-II/LC3-I protein levels with ΔIntegral IOP calculated from the last 6-week IOP measurements prior to tissue dissection (n = 9; five 4-month-old and four 18-month-old mice).

4-month-old mice. The band running between LC3-I and LC3-II, regarded as LC3-Int (~15 kDa), has been suggested to be a processing intermediate of LC3-I. We previously reported this band in the iridocorneal region of C57BL/6J.[25] Although the nature of the higher molecular band was not confirmed, it is presumed to correspond to pre-LC3, based on the molecular weight. Densitometric analysis of the bands showed a statistically significant decrease in LC3-Int (4 months: 1.054 ± 0.32, n = 5; 18 months: 0.154 ± 0.32, n = 4; P = 0.01, t-test) and lower LC3-I (4 months: 1.005 ± 0.2, n = 5; 18 months: 0.64 ± 0.4, n = 4; P > 0.05, t-test) protein levels in the angle region of 18-month-old mice compared to 4-month-old ones (Fig. 2B). A slight increase, although not statistically significant, in LC3-II was also observed (4 months: 1.101 ± 0.27, n = 5; 18 months: 1.367 ± 0.81, n = 4; P > 0.05, t-test). Most importantly, the LC3-

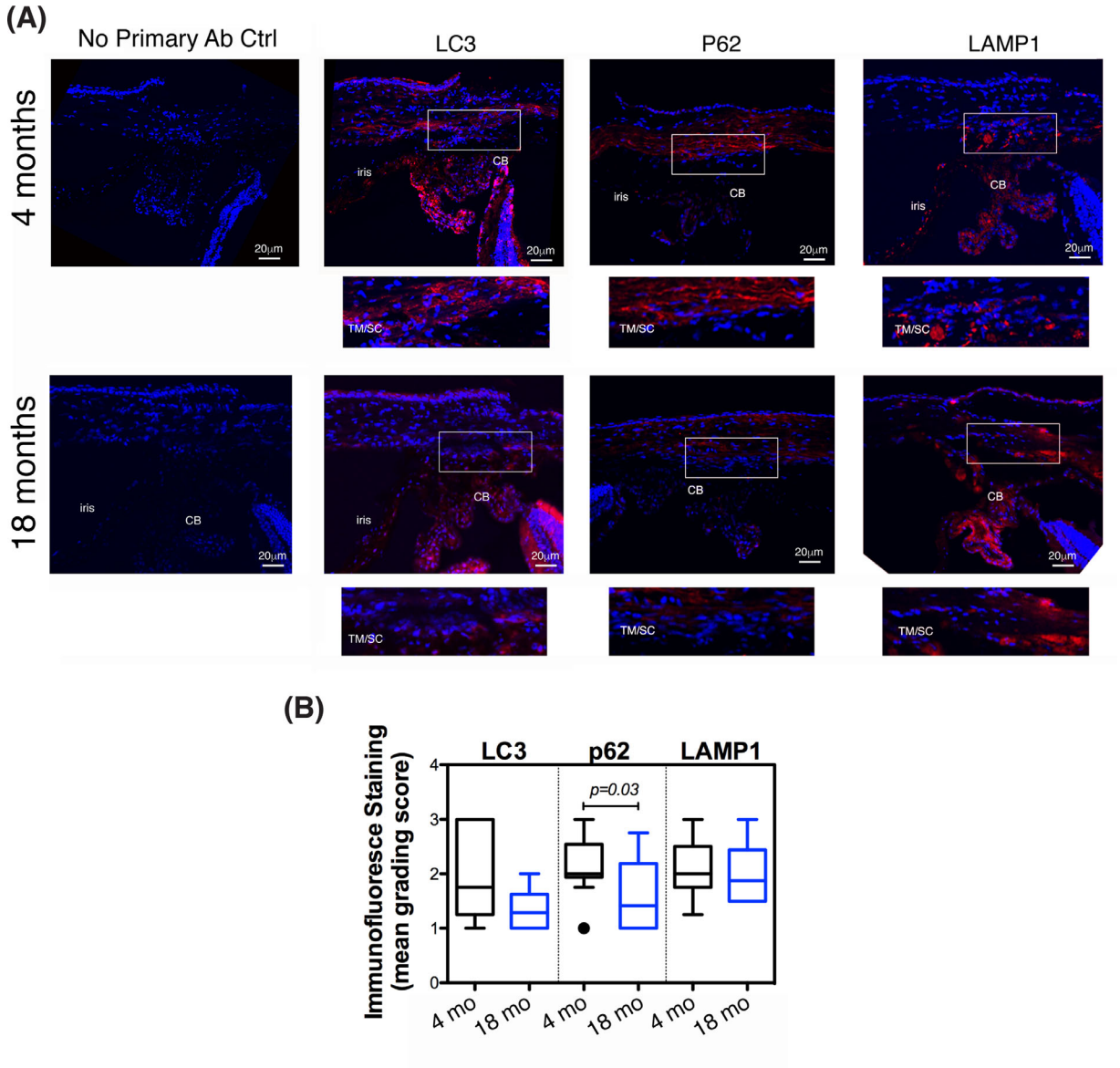

Figure 3. Qualitative expression of autophagy markers in the TM of 4-month-old and 18-month-old C57BL/6J mice. (**A**) Representative immunofluorescence staining of LC3, p62, and LAMP1 (*red fluorescence*). *Blue fluorescence* represents DAPI nuclear counterstaining. Insets show high-magnification images of the TM region. (**B**) Mean scoring values of IF staining in the TM/SC region graded in a masked fashion by three independent observers (*t*-test, $n_{4mo} = 11$, $n_{18mo} = 6$). CB, ciliary body.

II/LC3-I ratio, which measures autophagy activity, showed a highly significant increase in the iridocorneal region of the aging mice (4 months: 1.106 ± 0.21, $n = 5$; 18 months: 2.178 ± 0.10, $n = 4$; $P < 0.0001$, *t*-test) (Fig. 2C). Interestingly, as seen in Figures 2D and 2E, the LC3-II/LC3-I ratio, but not total LC3 level, correlated with cumulative IOP ($r = 82.79\%$, $P = 0.006$; $n = 9$, including five 4-month-old mice and four 18-month-old mice). We additionally compared by immunostaining in frozen sections the expression levels of LC3, the autophagy receptor p62, and the lysosomal marker LAMP1 in the TM/Schlemm's canal (SC) region between 4-month-old and 18-month-old mice (Fig. 3A). Sections were graded in a masked fashion by three independent observers, and mean scoring values were calculated (Fig. 3B). Overall, no significant qualitative or relative quantitative changes were observed for LC3 and LAMP1. A decrease in p62 staining in the TM/SC region of 18-month-old mice was observed (4 months: 2.117 ± 0.541, $n = 10$; 18 months: 1.597 ± 0.67, $n = 6$; $P = 0.03$, *t*-test).

Effect of Age and Transgene Expression in RGC Loss in Ocular Hypertensive Mice

We next evaluated whether age or transgene expression affects RGC loss in response to chronic IOP elevation. For this, we labeled whole retinal flat mounts with anti-Brn3a antibody and counted Brn3a-positive RGCs (Figs. 4A, 4B). As seen in Figure 4B, no significant changes in RGC count were observed between the injected and uninjected eye in 4-month-old C57BL/6J or GFP-LC3 mice. Also, in agreement with our previous study,[25] GFP-LC3 transgene expression

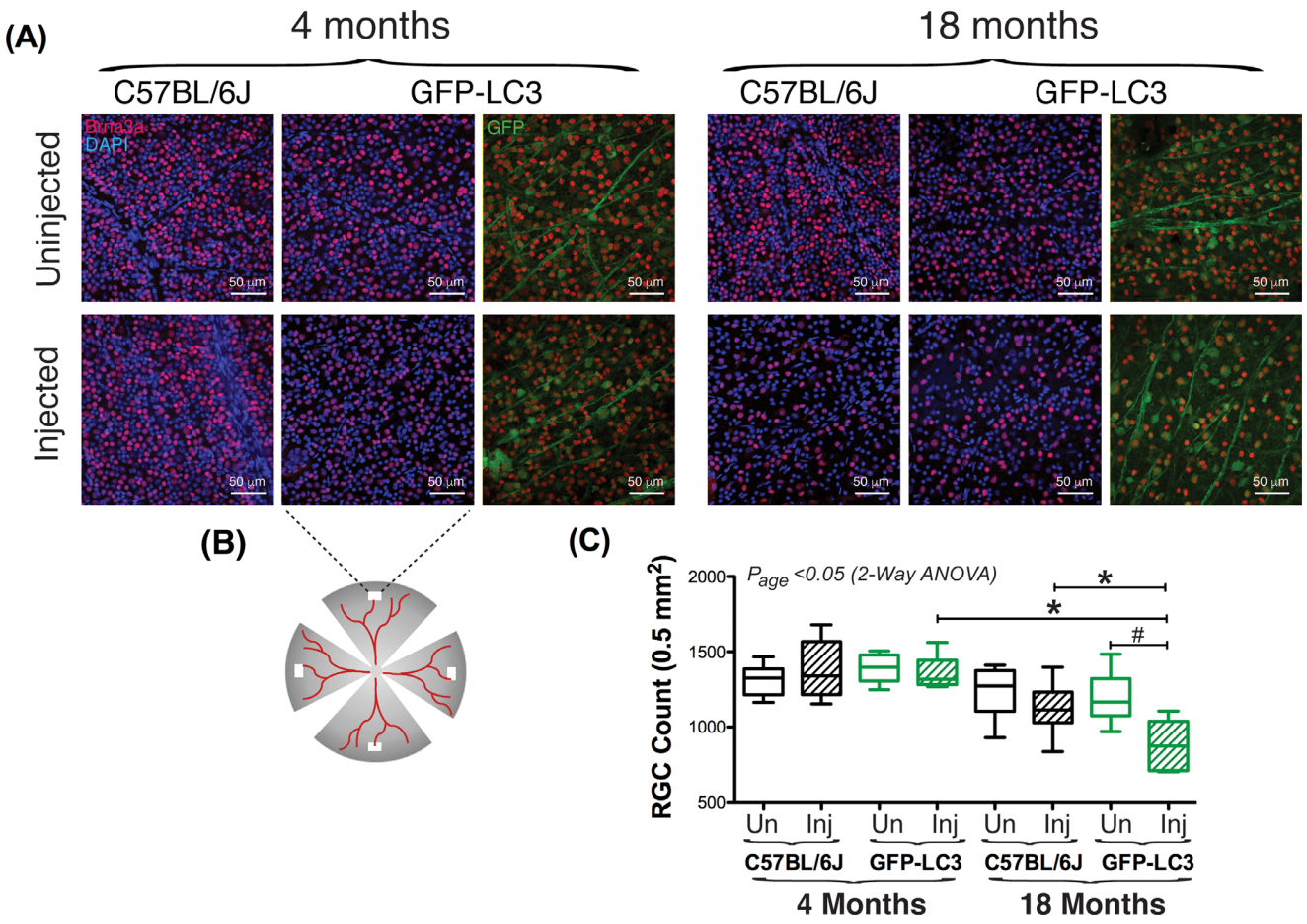

Figure 4. Effect of age and GFP-LC3 transgene in RGC loss in ocular hypertensive eyes. (**A**) Representative images from whole retinal flat mounts from 4-month-old and 18-month-old C57BL/6J and GFP-LC3 mice (uninjected and injected eyes) stained with anti-Brn3a (*red fluorescence*). *Green fluorescence* represents endogenous GFP-LC3 fluorescence; *blue fluorescence* represents nuclear DAPI staining. (**B**) Schematic drawing of flat mounts and placement of areas in which RGC counts were conducted. (**C**) Quantification of the number of Brn3a-positive cells. Data are the means ± SD. $^{*,\#}P < 0.05$: *2-way ANOVA with Bonferroni post hoc test, $^{\#}$paired *t*-test ($n_{4mo\text{-}C57BL/6J} = 6$, $n_{18mo\text{-}C57BL/6j} = 8$, $n_{4mo\text{-}GFP\text{-}LC3} = 5$, $n_{18mo\text{-}GFP\text{-}LC3} = 6$).

did not affect RGC viability. Two-way ANOVA analysis identified a statistically significant increase in RGC loss with aging in both uninjected eyes ($P < 0.02$) and injected eyes ($P < 0.05$). Interestingly, post hoc tests showed even greater RGC loss in the injected eyes of 18-month-old mice in combination with GFP-LC3: 4 $\text{months}_{\text{GFP-LC3-Inj}}$: 1393 ± 97, $n = 5$; 18 $\text{months}_{\text{GFP-LC3-Inj}}$: 1193 ± 172, $n = 6$ ($P < 0.05$); 18 $\text{months}_{\text{C57BL/6J-Inj}}$: 1123 ± 170, $n = 8$; 18 $\text{months}_{\text{GFP-LC3-Inj}}$: 873.2 ± 171, $n = 5$ ($P < 0.05$). In summary, our results indicate a role of aging and GFP-LC3 expression on RGC damage in response to IOP elevation. No significant correlation between cumulative IOP and RGC loss was found in any of the groups (not shown).

Autophagy in the RGC Layer of Aging and Ocular Hypertensive Eyes

Autophagy in the RGC layer of 4-month-old and 18-month-old C57BL/6J mice was investigated by monitoring LC3, p62, and LAMP1 levels by IF in frozen sections (Fig. 5). Interestingly, standardized relative quantification of IF staining showed increased LC3 in the RGC with aging (4 months: 0.476 ± 0.26, $n = 6$; 18 months: 0.844 ± 0.31, $n = 8$) and in the aging hypertensive eye (18 $\text{months}_{\text{Inj}}$: 0.844 ± 0.31, $n = 8$; 18 $\text{months}_{\text{Inj}}$: 1.183 ± 0.12, $n = 8$) ($P_{age} = 0.0046$, 2-way ANOVA) (Fig. 5B). No significant changes in p62 or LAMP1 were found in any of the experimental conditions, although a trend in higher p62 was observed in 18-month-old mice in response to IOP elevation (18 $\text{months}_{\text{Uninj}}$: 0.368 ± 0.26, $n = 6$; 18 $\text{months}_{\text{Inj}}$: 0.783 ± 0.59, $n = 6$).

Effect of Age and Transgene Expression in Axonal Degeneration in Ocular Hypertensive Mice

The effect of aging and/or transgene expression in axonal degeneration in response to elevated IOP was evaluated by conducting axon count in cross-sectional areas of the myelinated segment of the ON (Fig. 6). As seen in Figure 6B, no changes in total axon number were observed with aging or GFP-LC3 transgene expression in the uninjected eyes. A decrease in axon count was found in the injected eye when compared to the contralateral non-injected eye in all the groups; however, statistical significance was just reached in the 18-month-old mice (18 $\text{months}_{\text{C57BL/6J-uninj}}$:

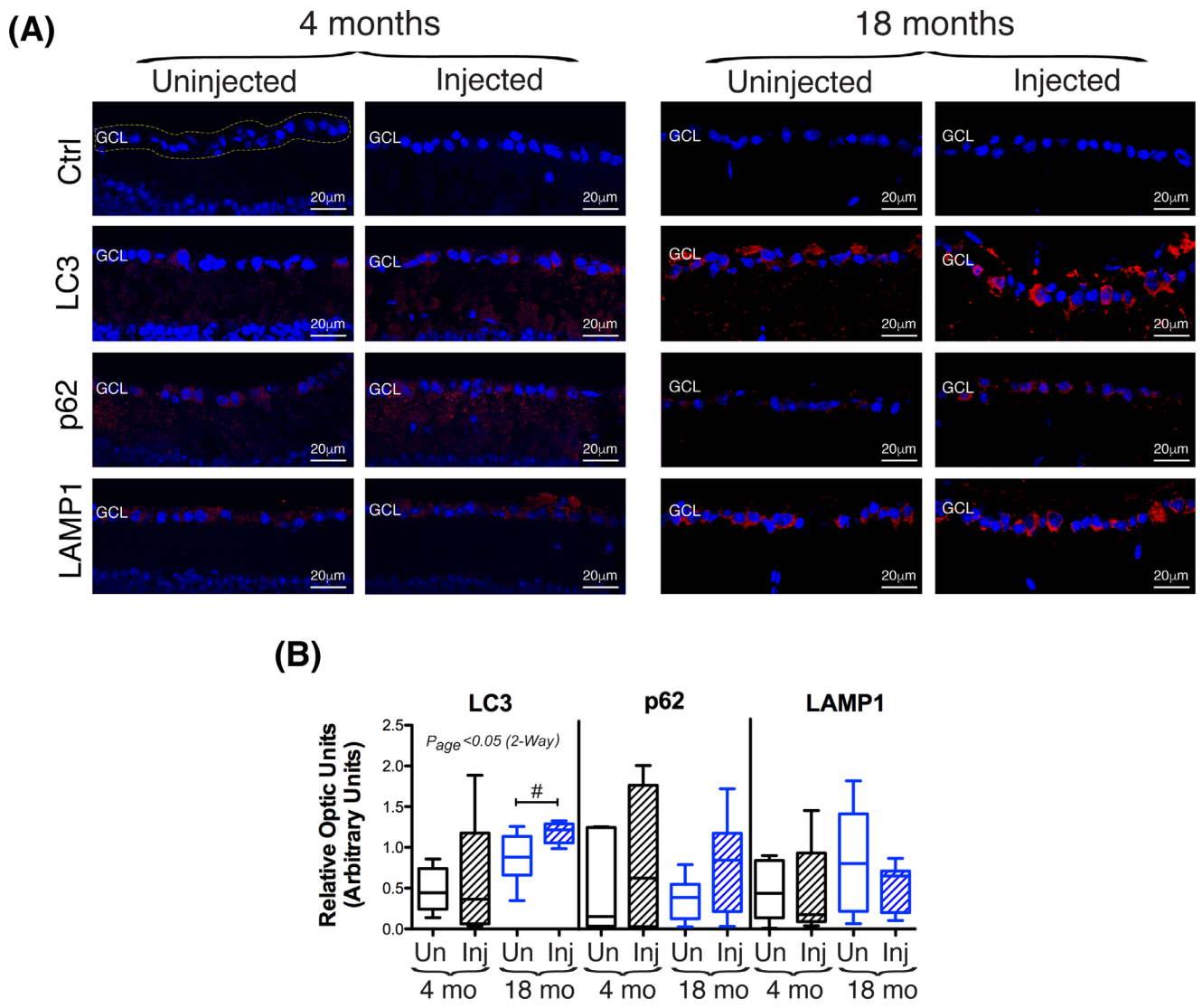

Figure 5. Autophagy in the GCL of aging and ocular hypertensive eye. (**A**) Representative immunofluorescence staining of LC3, p62, and LAMP1 (*red fluorescence*) in the GCL of injected and uninjected eyes in 4-month-old and 18-month-old C57BL/6J mice. *Blue fluorescence* represents nuclear DAPI counterstaining. The region of interest is delineated in *yellow*. (**B**) Standardized relative quantification of immunofluorescence staining in the region of interest. Data are the means ± SD. Two-way ANOVA with Bonferroni post hoc test; #paired *t*-test ($n_{4mo\text{-}C57BL/6J} = 6$, $n_{18mo\text{-}C57BL/6J} = 8$).

47,299 ± 7080 vs. 18 months$_{C57BL/6J\text{-}Inj}$: 38,749 ± 5473, $n = 6$, $P = 0.04$, paired *t*-test; 18 months$_{GFP\text{-}LC3\text{-}uninj}$: 41,726 ± 4341 vs. 18 months$_{GFP\text{-}LC3\text{-}Inj}$: 29,723 ± 4839, $n = 9$, $P = 0.006$, paired *t*-test). A statistically significant increase in axon loss was also identified with aging in the injected eyes ($P = 0.006$, 2-way ANOVA). Furthermore, pairwise analysis revealed more extensive axon loss in 18-month-old hypertensive GFP-LC3 mice compared to their respective C57BL/6J control ($P < 0.05$), similar to our previous findings in DBA/2J mice.[25] As in that case, autophagic structures were observed in degenerating axons (Fig. 6).

Discussion

Here, we have investigated for the first time, to the best of our knowledge, the effect of aging and experimental chronic elevation of IOP on autophagy activity in the iridocorneal region, RGC bodies, and ON axons of C57BL/6J and GFP-LC3 mice. Our results indicate a dysregulation of autophagy in the TM and RGC somas with aging and in the experimental ocular hypertensive mice. Unilateral sclerosis of the TM via injection of hypertonic saline in the episcleral vein produced sustained elevation of IOP in rats and mice, with optic nerve damage resembling that in human glaucoma.[26] Although less extensively, this experimental model has been adapted and successfully used in mice.[27,28] In our study, effective IOP elevation was highly dependent on aging. Although most 18-month-old mice significantly developed mild or severe elevation in IOP with subsequent axonal degeneration and RGC loss following just a single injection, 4-month-old mice were refractory to high IOP. The majority of the 4-month-old mice displayed a low or mild rise in IOP even after three injections. Accordingly, no significant mean RGC or axon loss was observed. Because it was not within the scope of this particular study, we did not follow up on such resistance to experimental IOP elevation in the 4-month-old mice.

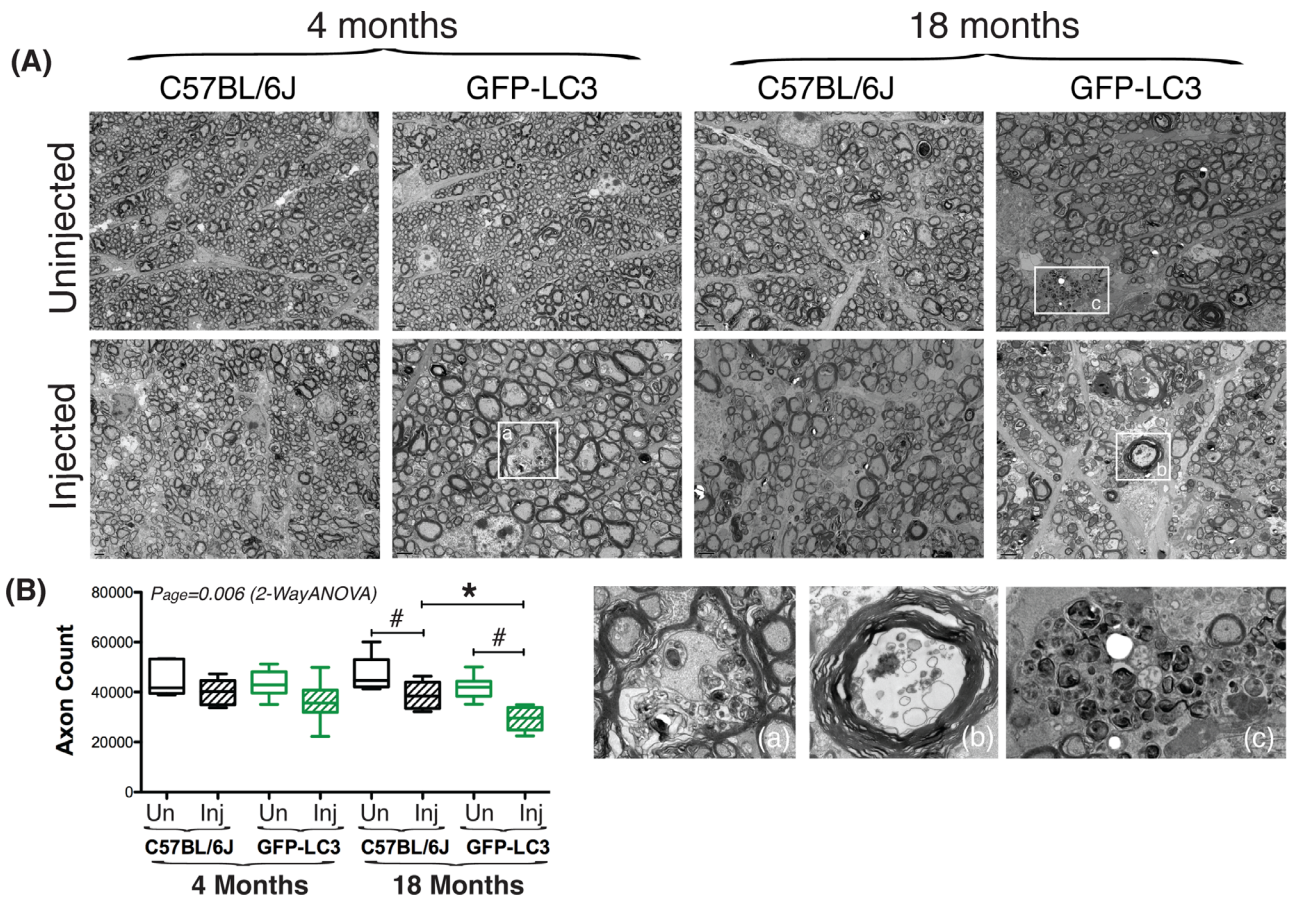

Figure 6. Effect of age and GFP-LC3 transgene in axonal degeneration in ocular hypertensive eyes. (**A**) Representative transmission electron micrographs of cross-sectional areas of the myelinated segment of the ONs in C57BL/6J and GFP-LC3 mice (4-month-old and 18-month-old, injected and uninjected eyes). Insets represent higher magnification images of autophagic structures in degenerating axons. (**B**) Total axon number counts. Data are the means ± SD. $^{*,\#}P < 0.05$: *2-way ANOVA with Bonferroni post hoc test, $^{\#}$paired *t*-test ($n_{4\text{mo-C57BL/6J}} = 6$, $n_{18\text{mo-C57BL/6J}} = 8$, $n_{4\text{mo-GFP-LC3}} = 6$, $n_{18\text{mo-GFP-LC3}} = 9$).

The hypertonic saline model relies upon scarring of the TM to a degree that it impedes aqueous humor outflow. It is plausible that the loss in regenerative potential typically associated with aging plays a role or predisposes to the development of sclerotic lesion in response to the saline injection. Similar regenerative loss might be responsible for the progressive increase in IOP with age, also reported by other groups.[29,30] Unfortunately, scarring of the TM was not evaluated to confirm whether differences between 4-month-old and 18-month-old mice existed. It is currently unknown whether this resistance to IOP elevation can be extended to other experimental glaucoma models. To our knowledge, this is the only study in which the impact of aging on the generation of experimental mouse hypertensive model has been investigated. In a recent work, Kimball et al.[31] examined axonal fragmentation in an ex vivo explant model of C57BL/6J mice (4 months old and 14 months old) exposed to chronic IOP by anterior microbead injection, but no IOP data were reported.

Dysregulation of autophagy with aging is believed to be one of the underlying mechanisms associated with the onset or progression of age-related diseases, especially in post-mitotic tissues such as the TM, with low proliferative rates. Our data showed changes in autophagy markers in the iridocorneal and TM tissues from 18-month-old mice compared to 4-month-old mice. Western blot analysis revealed decreased levels of LC3-I and the intermediate form LC3-Int but an overall statistically significant increase in the LC3-II/LC3-I ratio, which measures autophagy activity, in the 18-month-old mice. Lower levels of the autophagic flux indicator p62, with no significant changes in LAMP1 and total LC3, were detected by IF. As discussed in our previous work,[25] accurate quantification of autophagy in the murine outflow pathway is challenged by technical limitations in tissue dissection and effective markers to monitor the dynamic nature of autophagy *in vivo* or in dissected tissues. Although higher LC3-II/LC3-I ratios in combination with lower p62 levels might suggest higher autophagy activity, the expression of p62 is known to decline with aging in mice.[32] Indeed, p62 knockout mice showed premature signs of aging and reduced lifespan.[32] Alternatively, elevated LC3-II/LC3-I ratios with no changes in lysosomal content might imply diminished autophagy. Despite those limitations and potential interpretations, our data clearly indicate dysregulation of autophagy in the aging TM.

Higher expression levels of LC3 with aging were also observed in RGC somas of non-injected normotensive and even greater in the hypertensive eyes. The fact that no significant quantitative or qualitative differences in

autophagy markers were seen in the saline-injected eyes in 4-month-old mice most likely relates to their resistance to IOP elevation and emphasizes the relevance of IOP in autophagy activity in RGCs. Thus, the observed correlation between LC3-II/LC3-I ratio and IOP in the TM, although novel, is not entirely unexpected. Previous work from our laboratory reported the quick activation of autophagy in response to mechanical stress and high pressure.[33] Elevated LC3-II levels and the presence of autophagic bodies were observed in TM cells from porcine eyes when subjected to 30 mm Hg for 30 minutes. High LC3-II levels were also observed in the iridocorneal region and RGC layer of the spontaneous ocular hypertensive mice DBA/2J.[25] Altogether, these findings strongly indicate a relationship between autophagy and IOP.

Expression of GFP-LC3 transgene in the DBA/2J background caused higher magnitudes of IOP elevation and RGC loss, as well as dramatic axonal degeneration.[25] Interestingly, a similar neurodegenerative effect of GFP-LC3 was observed in our experimental hypertensive model. Saline-injected eyes of 18-month-old GFP-LC3 mice showed significantly increased RGC death and axon loss compared to their respective C57BL/6J controls. Also, as in the case of DBA/2J::GFP-LC3 mice, RGC axonal degeneration was accompanied by the presence of autophagic structures. Because this degenerative effect of GFP-LC3 was seen in 18-month-old, but not 4-month-old, mice, we believe it is related to the accumulated exposure to elevated IOP and, as discussed earlier, a decline and/or dysregulated stress response mechanism with aging. In this scenario, it is certainly reasonable to speculate the overactivation of autophagy triggered by a combined effect of sustained IOP elevation signaling and greater LC3 availability. This is supported by the occurrence of large autophagic structures in the degenerating axons of hypertensive GFP-LC3 eyes. Whether this represents "autophagic cell death" or "cell death with autophagy," as an attempt of the cell to induce autophagy as a survival pathway to ward off immediate damage,[34,35] cannot be determined but these findings add to the increasing body of literature linking autophagy with neurodegeneration in glaucoma.[20–24]

In summary, our results indicate dysregulation of autophagy in the TM and retinal tissues with aging and suggest that such dysregulation of autophagy contributes to neurodegeneration in glaucoma. Tools are currently being generated in our laboratory to better understand the nature and dynamics of such dysregulation and to more precisely evaluate the role of autophagy in the pathological processes of glaucoma.

Acknowledgments

The authors thank Ying Hao at the electron microscopy unit at Duke University, Department of Ophthalmology, for EM sample preparation.

Funding was provided by grants from the National Eye Institute, National Institutes of Health (EY026885, EY027733, EY005722), by a Brightfocus Foundation Glaucoma Research Award, and by a Research to Prevent Blindness Unrestricted Grant.

Disclosure: **A. Nettesheim,** None; **A. Dixon,** None; **M.S. Shim,** None; **A. Coyne,** None; **M. Walsh,** None; **P.B. Liton,** None

References

1. Tombran-Tink J, Barnstable CJ, Shields MB, eds. *Mechanisms of the glaucomas: disease processes and therapeutic modalities*. Totowa, NJ: Humana Press; 2008.
2. Chen DF, Cho K-S. Optic neuropathy and ganglion cell degeneration in glaucoma: mechanisms and therapeutic strategies. In: Tombran-Tink J, Barnstable CJ, Shields BM, eds. *Mechanisms of the glaucomas*. Totowa, NJ: Humana Press; 2008:393–423.
3. Beckman KB, Ames BN. The free radical theory of aging matures. *Physiol Rev*. 1998;78:547–581.
4. Cuervo AM. Autophagy and aging: keeping that old broom working. *Trends Genet*. 2008;24:604–612.
5. Levine B, Kroemer G. Autophagy in the pathogenesis of disease. *Cell*. 2008;132:27–42.
6. Huang J, Klionsky DJ. Autophagy and human disease. *Cell Cycle*. 2007;6:1837–1849.
7. Cuervo AM, Bergamini E, Brunk UT, Dröge W, Ffrench M, Terman A. Autophagy and aging: the importance of maintaining "clean" cells. *Autophagy*. 2005;1:131–140.
8. Koch JC, Lingor P. The role of autophagy in axonal degeneration of the optic nerve. *Exp Eye Res*. 2015;144:81–89.
9. Liton PB. The autophagic lysosomal system in outflow pathway physiology and pathophysiology. *Exp Eye Res*. 2015;144:29–37.
10. Munemasa Y, Kitaoka Y. Autophagy in axonal degeneration in glaucomatous optic neuropathy. *Prog Retin Eye Res*. 2015;47:1–18.
11. Wang Y, Huang C, Zhang H, Wu R. Autophagy in glaucoma: crosstalk with apoptosis and its implications. *Brain Res Bull*. 2015;117:1–9.
12. Porter K, Hirt J, Stamer WD, Liton PB. Autophagic dysregulation in glaucomatous trabecular meshwork cells. *Biochim Biophys Acta*. 2015;1852:379–385.
13. Russo R, Nucci C, Corasaniti MT, Bagetta G, Morrone LA. Autophagy dysregulation and the fate of retinal ganglion cells in glaucomatous optic neuropathy. *Prog Brain Res*. 2015;220:87–105.
14. Frost LS, Mitchell CH, Boesze-Battaglia K. Autophagy in the eye: implications for ocular cell health. *Exp Eye Res*. 2014;124:56–66.
15. Porter K, Hirt J, Stamer WD, Liton PB. Autophagic dysregulation in glaucomatous trabecular meshwork cells. *Biochim Biophys Acta*. 2015;1852:379–385.
16. Porter K, Nallathambi J, Lin Y, Liton PB. Lysosomal basification and decreased autophagic flux in oxidatively stressed trabecular meshwork cells: implications for glaucoma pathogenesis. *Autophagy*. 2013;9:581–594.
17. Liton PB, Lin Y, Luna C, Li G, Gonzalez P, Epstein DL. Cultured porcine trabecular meshwork cells display altered lysosomal function when subjected to chronic oxidative stress. *Invest Ophthalmol Vis Sci*. 2008;49:3961–3969.
18. Pulliero A, Seydel A, Camoirano A, Saccà SC, Sandri M, Izzotti A. Oxidative damage and autophagy in the human trabecular meshwork as related with ageing. *PLoS One*. 2014;9:e98106.
19. He JN, Zhang SD, Qu Y, et al. Rapamycin removes damaged mitochondria and protects human trabecular meshwork (TM-1) cells from chronic oxidative stress. *Mol Neurobiol*. 2019;56:6586–6593.
20. Rodríguez-Muela N, Germain F, Mariño G, Fitze PS, Boya P. Autophagy promotes survival of retinal ganglion cells after optic nerve axotomy in mice. *Cell Death Differ*. 2011;19:162–169.
21. Deng S, Wang M, Yan Z, et al. Autophagy in retinal ganglion cells in a rhesus monkey chronic hypertensive glaucoma model. *PLoS One*. 2013;8:e77100.

Investigative Ophthalmology & Visual Science

22. Knöferle J, Koch JC, Ostendorf T, et al. Mechanisms of acute axonal degeneration in the optic nerve in vivo. *Proc Natl Acad Sci U S A*. 2010;107:6064–6069.
23. Park HYL, Kim JH, Park CK. Activation of autophagy induces retinal ganglion cell death in a chronic hypertensive glaucoma model. *Cell Death Dis*. 2012;3:e290–e290.
24. Su W, Li Z, Jia Y, Zhuo Y. Rapamycin is neuroprotective in a rat chronic hypertensive glaucoma model. *PLoS One*. 2014;9:e99719.
25. Hirt J, Porter K, Dixon A, McKinnon S, Liton PB. Contribution of autophagy to ocular hypertension and neurodegeneration in the DBA/2J spontaneous glaucoma mouse model. *Cell Death Discov*. 2018;4:14.
26. Morrison JC, Moore CG, Deppmeier LM, Gold BG, Meshul CK, Johnson EC. A rat model of chronic pressure-induced optic nerve damage. *Exp Eye Res*. 1997;64:85–96.
27. Kipfer-Kauer A, McKinnon SJ, Frueh BE, Goldblum D. Distribution of amyloid precursor protein and amyloid-beta in ocular hypertensive C57BL/6 mouse eyes. *Curr Eye Res*. 2010;35:828–834.
28. Walsh MM, Yi H, Friedman J, et al. Gene and protein expression pilot profiling and biomarkers in an experimental mouse model of hypertensive glaucoma. *Exp Biol Med (Maywood)*. 2009;234:918–930.
29. Cone FE, Steinhart MR, Oglesby EN, Kalesnykas G, Pease ME, Quigley HA. The effects of anesthesia, mouse strain and age on intraocular pressure and an improved murine model of experimental glaucoma. *Exp Eye Res*. 2012;99:27–35.
30. Millar JC, Phan TN, Pang I-H, Clark AF. Strain and age effects on aqueous humor dynamics in the mouse. *Invest Ophthalmol Vis Sci*. 2015;56:5764–5776.
31. Kimball EC, Jefferys JL, Pease ME, et al. The effects of age on mitochondria, axonal transport, and axonal degeneration after chronic IOP elevation using a murine ocular explant model. *Exp Eye Res*. 2018;172:78–85.
32. Kwon J, Han E, Bui C-B, et al. Assurance of mitochondrial integrity and mammalian longevity by the p62-Keap1-Nrf2-Nqo1 cascade. *EMBO Rep*. 2012;13:150–156.
33. Porter KM, Jeyabalan N, Liton PB. MTOR-independent induction of autophagy in trabecular meshwork cells subjected to biaxial stretch. *Biochim Biophys Acta*. 2014;1843:1054–1062.
34. Kriel J, Loos B. The good, the bad and the autophagosome: exploring unanswered questions of autophagy-dependent cell death. *Cell Death Differ*. 2019;26:640–652.
35. Denton D, Kumar S. Autophagy-dependent cell death. *Cell Death Differ*. 2019;26:605–616.

Investigative Ophthalmology & Visual Science